Hyaluronic Acid−(Hydroxypropyl)cellulose Blends: A Solution and Solid State Study

Vipul Davè, Monica Tamagno, and Bonaventura Focher*

Stazione Sperimentale per la Cellulosa, Carta e Fibre Tessili Vegetali ed Artificiali, Piazza L. Da Vinci 26, 20133 Milano, Italy

Enrico Marsano

Istituto di Chimica Industriale, Università di Genova, Corso Europa 30, 16132 Genova, Italy

Received June 24, 1994; Revised Manuscript Received January 5, 1995®

ABSTRACT: We report a study of the compatibility of a system involving a flexible polymer, hyaluronic acid (HA), and a semirigid polymer, (hydroxypropyl)cellulose (HPC). The phase diagram of ternary mixtures composed of HA, HPC, and H_2O showed a homogeneous solution at an overall polymer concentration lower than $C_p \approx 15\%$, but when the concentration was increased, two demixing areas were evidenced: the first (range C_p 15−21%) corresponds to an equilibrium between two isotropic phases, while the second (over $C_p = 21\%$) represents the coexistence of a HPC mesophase with an isotropic phase of both polymers. In contrast, optical and electron microscopy observations as well as X-ray, FT-Raman, DSC, and DMTA experiments carried out on blended films showed complete HPC/HA compatibility in all the compositions. DMTA experiments revealed a single glass transition temperature (T_g); its dependence as a function of composition was analyzed by Kwei's equation. Different values were found for dry and 65% relative humidity (RH) conditioned samples, suggesting the important role of water as a plasticizer in HPC/HA blends.

Introduction

The connective tissue in mammalians consists of an interpenetrating continuous network of various polysaccharides and collagen fibrils that form a solid three-dimensional matrix where organs and bones are located. The major component is hyaluronic acid (HA) that acts as a cementing substance, forming a jelly-like matrix between the cells of various tissues such as skin, tendons, muscles, and cartilage.[1,2] Chemically, HA is an unbranched polysaccharide consisting of alternating residues of β-(1,3)-D-glucuronic acid and β-(1,4)-D-*N*-acetylglucosamine.[3] Segmental mobility of the HA chains is more restricted than for similar polysaccharides owing to a local stiffness induced by the existence of intramolecular hydrogen bonds. This stiffness is responsible for the large hydrated volume of the HA chains, keeping the neighboring tissues swollen and maintaing HA chain integrity.[4] The fact that HA is soluble under physiological conditions, and undergoes enzymatic degradation in localized zones like lymph nodes, precludes the preparation of stable devices able to reproduce environments suitable for accelerating cell adhesion and mobility and thus prevents the growth of some tissues like skin and tendons.[3] Hence chemical reticulation of the HA chains[5] and the preparation of HA derivatives such as esters have been proposed,[6] but the chemical modification of HA might have a negative effect on its biological function.

In recent years polymeric blends have been recommended as a way of improving polymer properties without markedly changing the structure and function of the polymers themselves. Thus the presence of the blend of a polymer that is not biodegradable under physiological conditions could reduce the susceptibility of HA to enzymatic attack.

The purpose of the present investigation has been to study the compatibility of HA with another biocompatible polysaccharide such as (hydroxypropyl)cellulose (HPC). Since most concentrations of the examined solutions of the blend show thermodynamic immiscibility, it is of interest to ascertain whether partial miscibility can be reached under nonequilibrium conditions by freezing some molecular arrangements of the polymers through the casting procedure used in film preparation. This study was performed by using different techniques (optical and electron microscopy, X-ray, FT-IR and FT-Raman, DSC, and DMTA) to study the strength of the molecular interactions between the polymers, through T_g blend composition relationships.

Experimental Section

Materials. Hyaluronic acid (HA) was obtained from Fidia S.p.A., Abano Terme, Italy, with $M_w = 146\,000$ as determined by gel permeation chromatography. The (hydroxypropyl)-cellulose (HPC) Klucel LF sample was kindly supplied by Hercules Inc. (M_w = 100 000, molecular substitution, MS, equal to 4; data reported by the supplier) and was used as received.

Phase Diagram. We followed the technique described by Bianchi et al.[7] to prepare the ternary phase diagram. Ternary mixtures covering an overall polymer concentration (C_p) ranging between 10% and 70% were prepared by dissolving weighed amounts of HA and HPC in water. The system was allowed to reach equilibrium by mechanical stirring for 3−4 weeks. As the solutions were very viscous, mechanical stirring was necessary for 3−4 weeks at room temperature in order to reach equilibrium. Separation of the coexisting phases was achieved by centrifugation at 30 000 rpm (g = 81 300) for about 200 h. The composition of the two phases was determined by using weighed aliquots of each phase. Each aliquot was freeze-dried and weighed. The quantitative amount of HPC and HA in the precipiate was determined by methanol (nonsolvent for HA) extraction.

To compare the theoretical and experimental results the concentrations, expressed as polymer volume fraction, were converted into C_p, this being calculated by using the following values of the specific volume: $V_{sp\,HPC} = 0.8849$, $V_{sp\,HA} = 0.6896$, $V_{sp\,H_2O} = 1$; their addivity was assumed.

* To whom all correspondence should be addressed.
® Abstract published in *Advance ACS Abstracts,* April 1, 1995.

0024-9297/95/2228-3531$09.00/0

Optical and Scanning Electron Microscopy (SEM). Optical observations were carried out using an Ortholux Leitz polarizing microscope equipped with a Mettler FP 82 hot stage system. The study was made between 25 and 250 °C. Electron microscopy was performed on a Philips 515 scanning electron microscope with an accelerating voltage of 12 kV. Fracture surfaces were formed in liquid nitrogen. To avoid electron charging effects, the films were sputter coated by pure gold for 1 min in an Edwards S150 sputter coater.

Film Preparation. Stock solutions (2%) of HPC and HA were prepared in distilled water. The blended solutions of HPC and HA were prepared by mixing the stock solutions in different proportions. To prepare the films with nearly the same thicknesses, 25 mL of the blended solutions was poured onto glass molds that were then kept in a hood for more than 2 days to evaporate the solvent. The dry films were then peeled off and dried in a vacuum oven at 60 °C for 48 h. The average film thickness, measured by a Lorentzen and Wettres Micrometer, was 50 μm. The dry films were kept in a conditioned room (65% RH, 20 °C) for 48 h.

Wide Angle X-ray Diffraction (WAXD). The wide angle X-ray patterns of the films were recorded using Ni-filtered Cu Kα radiation from a Siemens D-500 diffractometer with a Siemens FK 60-10, 2000 W copper tube. The instrument was equipped with a scintillator counter and a linear amplifier. The set conditions were 40 kV and 18 mA with a scanning rate of 2°/min. X-ray diffractograms at different temperatures were recorded by using a TTK-temperature camera (Anton Paar K.G.). These diffractograms were recorded in the range 25–210 °C.

FT-IR and FT-Raman Spectroscopy. Infrared spectra were obtained with a Bruker (Karlsruhe) IFS 66 FT-IR spectrometer on films prepared from a 0.3% solution in Teflon molds; 32 scans were accumulated for each sample, with a resolution of 4 cm^{-1}. The Raman spectra of the films were obtained with a Bruker FRA 106 Raman accessory for an IFS 66 FT-IR spectrometer using a laser power of 260 mW; 3000–4000 scans were accumulated for each sample, with a resolution of 8 cm^{-1}.

Differential Scanning Calorimetry (DSC). Calorimetric measurements were carried out using a Perkin-Elmer DSC 4 in a nitrogen atmosphere on samples (10–12 mg) pretreated at 150 °C for 30 min and rapidly cooled in liquid nitrogen before measurements. The scan was carrired out on the films at 20 °C/min from −20 to +300 °C. Annealing treatments on some samples were performed at 120 °C for 24 h.

Dynamic Mechanical Thermal Analysis (DMTA). The dynamic storage modulus (E'), loss modulus (E''), and mechanical loss tangent δ were measured with a Polymer Laboratories Mk III DMTA at 5 Hz in the tensile mode. The temperature was increased at a rate of 3 °C/min from −100 to +130 °C. Due to the excessive softness of both blend components at temperatures beyond 120 °C, it was not possible to measure the dynamic mechanical properties near the HPC softening point. The typical specimen size for measurement was 15 mm × 5 mm. The experiments were carried out on specimens dried at 60 °C under vacuum for about 48 h, and on specimens exposed to 65% RH.

Results and Discussion

Solution Study. Table 1 shows the results of the optical observations of a solution of HPC/HA mixtures of different concentrations and compositions using the optical microscope in both normal and polarized light. A composition analysis of the conjugated phases was carried out for several mixtures; the results are reported in Table 2. For binary mixtures of HPC/H_2O the critical concentration (C_p') at which the birefringent liquid crystalline phase (lc) occurred was 39%. The concentration (C_p'') at which the binary mixture HPC/H_2O was completely anisotropic is 47%, in close agreement with values obtained by Ciferri et al.[8] For concentrations between C_p' and C_p'' the mixture was biphasic.

Table 1. Overall Composition of Ternary Mixtures

mixtures	$C_{p,HPC}$, %	$C_{p,HA}$, %	(HPC + HA), %	appearance after equilibrium
A	5.1	5.1	10.2	homoeneous, isotropic
B	7.6	7.7	15.3	homogeneous, isotropic
C	12.5	5.4	17.9	homogeneous, isotropic
D	5.1	11.9	17.0	biphasic, isotropic
E	7.9	8.0	15.9	biphasic, isotropic
F	14.7	6.3	21.0	biphasic, isotropic
G	25.5	6.4	31.9	biphasic, isotropic, anisotropic
H	15.1	14.9	30.0	biphasic, isotropic, anisotropic
I	20.0	19.9	39.9	biphasic, isotropic, anisotropic
L	34.9	15.0	49.9	biphasic, isotropic, anisotropic
M	48.0	12.0	60.0	biphasic, isotropic, anisotropic

Table 2. Composition of Conjugated Phases

	phase I		phase II	
mixtures	$C_{p,HPC}$, %	$C_{p,HA}$, %	$C_{p,HPC}$, %	$C_{p,HA}$, %
I	52.0	0.3	1.8	30.1
L	60.0	0.6	3.7	35.4
M	66.5	0.9	2.9	39.6

With regard to the behavior of HA in water no mesophase was formed, not even for a very highly concentrated solution (C_p = 60%).

The presence of a uronic acid in the repeating unit of HA gives this polysaccharide the properties of a polyelectrolyte.[9–11] The total persistence length for a polyelectrolyte (q_t) is due to the sum of two contributions:[12]

$$q_t = q_{st} + q_e$$

q_{st} being due to the steric properties of the charged polymer, and q_e deriving from all the electrostatic interactions; note that q_e is inversely proportional to the salt and polymer concentrations.[9,10] For HA in the high ionic strength limit the literature reports values of q_t ranging from 40 to 87 Å.[9–13] The macromolecular chain, though not very rigid, should be stiff enough to stabilize a liquid crystalline phase, however, as already observed for other polysaccharide systems,[14] with q as high as 200 Å it is possible that lateral aggregation phenomena occur, thus affecting the value of the diameter of the rodlike aggregates and hence causing a decrease in the value of the axial ratio (X).[15] The axial ratio equals the ratio between the Kuhn segment ($K = 2q$) and the diameter, and X is the critical parameter in the formation of a mesophase; if $X < 6.5$, no liquid crystal phase can be observed and the polymer can be considered as a "flexible polymer".[16]

The ternary phase diagram (Figure 1) was constructed from data in Tables 1 and 2, respectively, which represent the overall polymer composition of the ternary mixtures and the composition of the conjugated phases. The indexes 1–3 refer to water, HPC, and HA, respectively. Binary mixtures HPC/H_2O, HA/H_2O, and HPC/HA are represented on the left-hand side, the right-hand side, and the base axis, respectively. It is possible to distinguish three regions (a–c) in the phase diagram. Region a corresponds to the dilute homogeneous isotropic solutions containing both components; the solutions are clear to the naked eye and under the microscope. The lower part of this region is bordered by the demixing curve. Region b corresponds to a biphasic system where separation in two isotropic phases, one rich in HPC and the other in HA, has occurred. Photo 1 shows an optical micrograph of this region. Region c corresponds to a biphasic area where an anisotropic solution or pure HPC and water is in equilibrium with

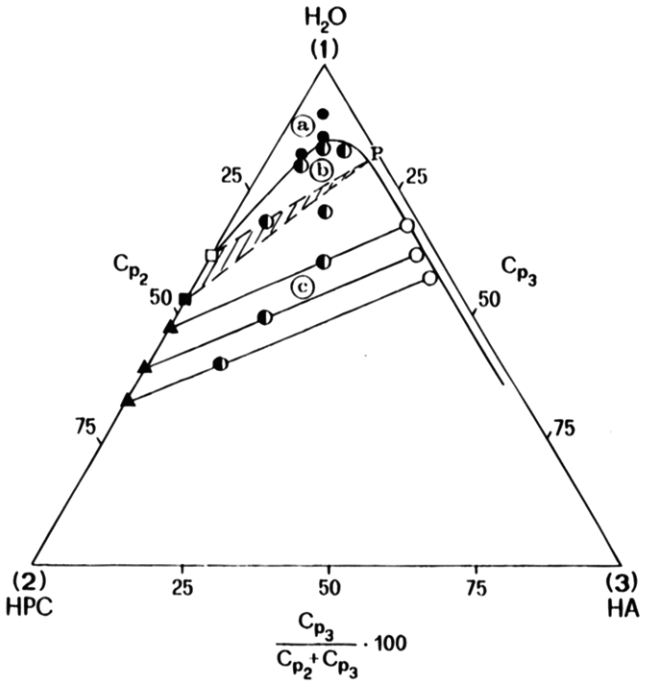

Figure 1. Ternary phase diagram for the system HPC/HA/H_2O; (●) overall composition of the monophasic solutions; (◐) overall composition of the biphasic mixtures; (○) composition of the conjugated isotropic; (▲) composition of the conjugated anisotropic phases; (□,■) limit concentration of the biphasic gap for HPC.[8]

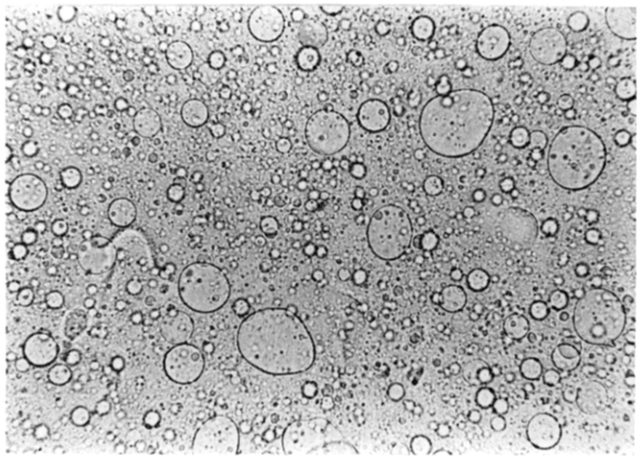

Photo 1. Optical micrograph of the 30/70 HPC/HA blend, C_p = 20.0% (region b).

an isotropic solution of HPC, HA, and water. Photo 2 shows an optical micrograph of this region. A dashed triangular area is outlined from the limit of the biphasic gap through to point P on the curve, a point determined by tracing a straight line through C_p' of HPC and C_p' of a ternary mixture (80% HPC–20% HA), until crossing the mixing curve. This dashed area was not clearly identified, as it is composed of three phases: one anisotropic, composed of HPC and water, and two isotropic, one of HPC/H_2O and the other of HPC/HA/H_2O. Such behavior is well-known for systems composed of rigid and flexible polymers.[17,18] Hence these experimental results confirm that it is reasonable to consider HA a "flexible" polymer; had HA behaved as a semirigid polymer a second three-phase area composed of an isotropic HA/H_2O phase and two anisotropic HA/H_2O and HPC/H_2O phases would have been observed.[18,19]

For the upper portion of the phase diagram (region b) it is evident that the separation between the two

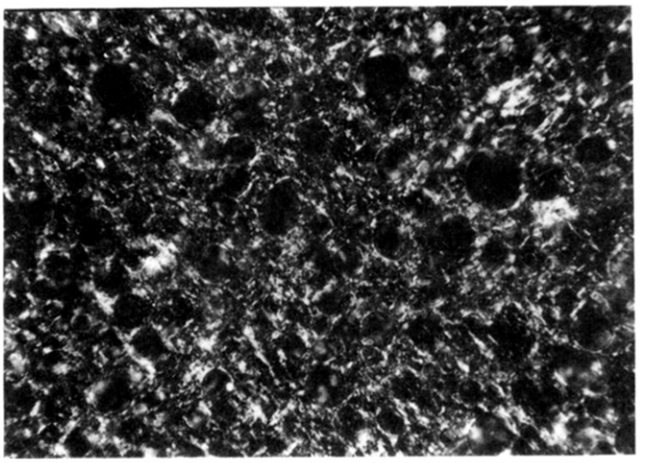

Photo 2. Optical micrograph of the 30/70 HPC/HA blend, C_p = 30.0% (region c).

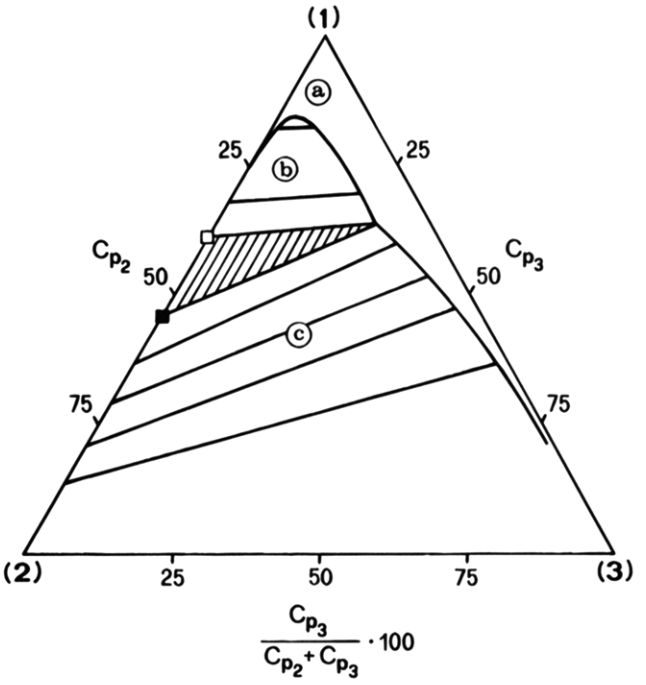

Figure 2. Theoretical phase diagram for a system composed of a semirigid polymer with a Kuhn chain formed of ten segments and a "flexible polymer" with a contour length of HA x_3 = 360 and an interaction parameter χ_{23} = 0.076; (a) homogeneous isotropic solution; (b) biphasic isotropic solution; (c) biphasic isotropic anisotropic solution. The dashed area is three-phasic: two isotropic and an isotropic solution.

polymers occurs in the isotropic phase. This behavior is in agreement with the theoretical evaluation of the interaction parameters calculated with the Hansen method[20] based on contributions from dispersion, polarity, and hydrogen bonds. A positive value of the interaction parameter was obtained (χ_{23} = 0.076), suggesting that a demixing process occurs at a certain concentration, as observed experimentally.

The theoretical phase diagram (Figure 2) was calculated according to Flory's theory[21] for a system composed of a semirigid polymer (HPC), a "flexible" one (HA) and a solvent (H_2O). For a quantitative comparison the ratio between the Kuhn segment and the diameter of HPC (axial ratio X_2) must be established.

The literature reports values of the axial ratio for HPC[22–25] ranging from 8 to 20, depending on both the solvent and the method used to evaluate the axial ratio. Note that the values of the experimental critical con-

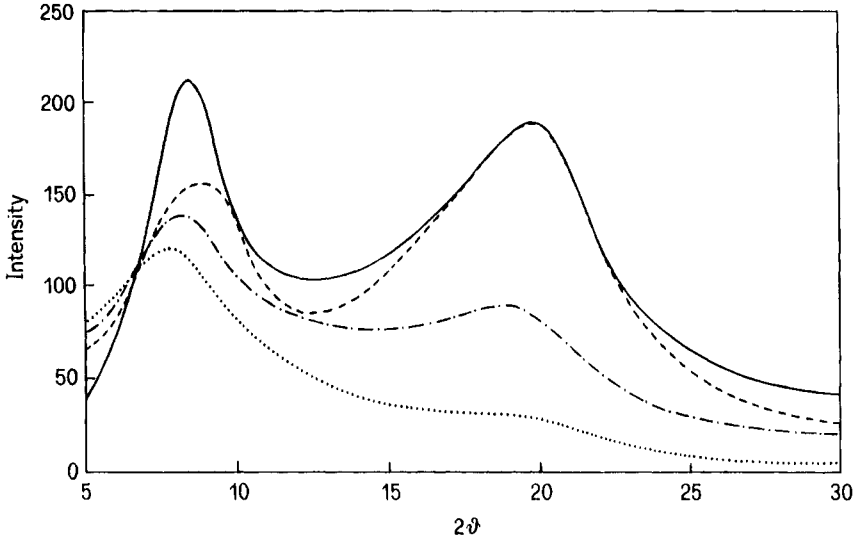

Figure 3. X-ray diffractograms of HPC at different temperatures (—) 25 °C; (- - -) 160 °C; (· — ·) 185 °C; (···) 210 °C.

centration ($C_{p'exp}$), larger than those expected on the basis of the axial ratio ($C_{p'theor}$) have already been reported,[23-25] $C_{p'theor}/C_{p'exp}$ ratios having been as high as 1.5–2.5.[25] To have the best fit of the experimental results, it was suggested to derive X_2 from the $C_{p'exp}$ using equations C2–C6 of ref 16. $X_2 = 20$ was obtained for HPC samples; thus for our HPC sample with a molecular weight of 100 000 there is a chain composed of ten Kuhn segments with an axial ratio equal to 20.

Actually, HA should also be considered a semirigid polymer; hence the axial ratio should equal the ratio between the Kuhn segment and the diameter. As reported above, the experimental phase behavior of this polymer does not show any formation of the liquid crystalline phase, neither in a binary system nor in a ternary one. This suggests that HA should be considered in the context of a flexible polymer, the X_3 value being derived from the ratio of the contour length and the chain diameter; thus $X_3 = DP l_o/d$ where DP = degree of polymerization, l_o = length of the repeating unit, and d = diameter. For HA we used DP = 386, l_o = 1.03 Å,[26] and d = 11 Å;[26] hence $X_3 = 360$. Differences between the theoretical and experimental diagrams could be ascribed to the strong molecular interactions of water with the polymers; such interactions were not considered in the theoretical diagram ($\chi_{12} = \chi_{13} = 0$). The entropy effect of the counterion, which increases the demixing entropy of the two polymers in a common solvent of high dielectric constant, could also play an important role in the discrepancies between the two diagrams.[27]

Solid State Study: HPC Characterization. The optical microscope was used to observe HPC films in polarized light, the samples being heated from 25 to 250 °C. At room temperature the films are birefringent. Increasing the temperature, you can observe the softening point at 130 °C, and after this there is flowing in the system, indicating a liquid crystalline phase. The birefingence completely disappears at 205 °C, because of the isotropization of the liquid crystalline phase.

The X-ray diffractograms of pure HPC film registered at different temperatures (Figure 3) show, at room temperature, the presence of diffused scattering at 20.3° (2θ) associated with the presence of a liquid crystalline structure[26] together with a more ordered phase 7.8° (2θ) indicated by Samuels[28] as an equatorial reflection (100). When the temperature increases, there is a decrease in the reflection intensity at 7.8° together with marked broadening and a shift toward smaller angles. On the other hand, the reflection at 20.3° shows no variation up to 160 °C while there is a decrease with increasing temperature until its disappearance, corresponding to the isotropization temperature (T_i) (210 °C) of the liquid crystalline phase.

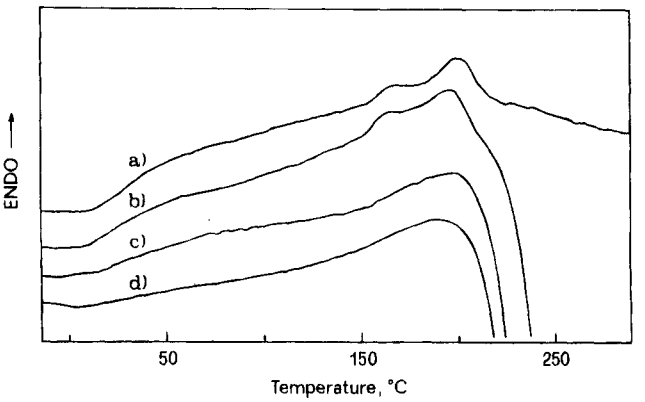

Figure 4. DSC curves of HPC/HA blends: (a) 100/0; (b) 75/25; (c) 25/75; (d) 0/100).

Furthermore, X-ray diffractograms of stretched fiber[29] recorded in the 25–100 °C range of temperature show some equatorial reflections ascribed to the presence of ordered regions that remain with no significant variations throughout the investigated temperature range.

Also the DSC analyses (Figure 4, trace a), in addition to the presence of a T_g event at around 30 °C, show a transition of weak intensity around 155 °C and a clear endothermic transition at 205 °C. In an effort to interpret these transitions, an analysis was made of samples that were first subjected to annealing at 120 °C for different times. As can be seen from Figure 5, increasing the annealing time (from 0 to 24 h) resulted in a well-defined melting at 155 °C, the increase in ΔH being associated with passing from 0.75 to 2.0 J/g. In contrast, the endotherm remains almost constant at T = 205 °C and ΔH = 3.6 J/g. These results, in agreement with the optical microscope observations in polarized light and the X-ray diffraction results, appear to show that the transition at 155 °C is associated with the melting of the ordered phase, probably a microcrystalline phase dispersed in the liquid crystalline phase that prevents the system from flowing. The endotherm at

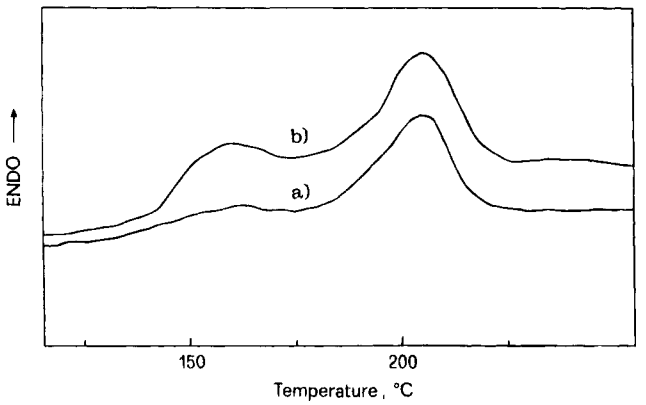

Figure 5. DSC curves of HPC after annealing treatment at 120 °C at different times (a) 0 h; (b) 24 h.

205 °C corresponds to the isotropization of the system rather than to its melting, as reported in the literature.[30,31] Rials et al. found analogous behavior for samples annealed at different temperatures and interpreted it in terms of variations of T_g.[31]

In an effort to have a deeper insight into HPC behavior with temperature, DMTA experiments, generally considered more sensitive than calorimetric ones to molecular motions,[30,32-34] were carried out. In DMTA spectra the T_g value is defined as either the tan δ peak temperature or the onset of the fall of the storage modulus E'. The temperature dependence of the mechanical loss tan δ of HPC dried film measurements (Figure 6) consists of three processes connected with the structure of the semicrystalline material. The low-temperature process γ, observed in several polysaccharides, was attributed to conformational variations due to local motions of either the main chain around the glycosidic linkage or the methylol groups of the glucosidic ring.[35] The γ process is observed at about −66 °C and can be attributed to the motions of both the backbone and the hydroxypropyl side chains.[30] The α_a process observed for HPC films at room temperature (ca. 30 °C) is commonly associated with a devitrification process of a glassy isotropic phase.[30] The process α_m, observed at higher temperature (ca. 120 °C) seems to reflect, according to microscope observations, a transition from a frozen anisotropic phase to a more mobile liquid crystalline phase throughout the melting of the crystalline zones. At freezing temperatures the storage modulus E' of the HPC films shows typical values (3−4) × 10^9 Pa) for a glassy state polymer. On an increase in temperature log E' first decreases smoothly and then falls to 5−25 °C, somewhat lower than the tan δ maximum. Finally, it drops sharply at about 120 °C in correspondence with the α_m process.

HA Characterization. The optical microscope observation of the HA film in polarized light showed no particular structure changes for temperatures of 25−250 °C. Degradation of the sample appeared around 240 °C.

The X-ray diffractograms of unstretched films did not reveal the presence of highly ordered zones, only superimposed reflection phases of low regularity. As seen in the literature, only the HA stretched films showed a high crystallinity and orientation, the structure having a double helix that can exist in both acid and physiological conditions.[36,37]

DSC analysis clearly evidenced an exothermic peak at 238 °C due to the degradation phenomenon (Figure 4, trace d), as previously observed.[38]

DMTA spectra for HA (Figure 7) showed the γ process at about −85 °C. The temperature dependence of tan δ resulted in a composite transition around room temperature constituted by a main transition at about 14 °C, associated with large-scale motion of the molecular chain segments (i.e. T_g transition). The initial storage modulus E' of HA films decreases slightly up to −22 °C, then shows a simple discontinuity around 25 °C, and finally shows an increase when the temperature is at about 50 °C. This phenomenon is common to other polysaccharides and has been considered to account for a strain-induced crystallization with an increase in the number of intermolecular and/or intramolecular hydrogen bonds before high-temperature relaxation phenomena occur.[31]

Blend Characterization. The existence of a liquid crystalline phase at room temperature has been shown by the optical microscope using polarized light in several of the HPC/HA mixtures. The presence of HA does not appear to interfere with the stability of the liquid crystalline phase until the HA content is about equal to 50% (Photos 3 and 4), for higher HA contents the birefringence disappears completely, suggesting the presence of completely amorphous structures. Furthermore, increasing the HA content in the mixture gradually raises the softening temperature.

The DSC thermograms of the films of HPC/HA blends are quite different from those of the pure components, as shown in Figure 4 (traces b and c.). The T_i transition of HPC in the blends disappears when the HA content is higher than 50%, while there is no indication of the T_g value. The HA decomposition temperature (T_d) was shown to be influenced by the presence of HPC in the blends, passing from 238 to 248 °C for the mixture containing 90% HPC.

To show any interactions between the two polymers at the molecular level, FT-IR and FT-Raman analyses were made. The IR analyses carried out on films of different blends showed no shift in the band frequencies of amide I (1655 cm^{-1}) and amide II (1569 cm^{-1}), or of the salt form of the carboxylic bands at 1615 (ν_a) and 1410 (ν_S) cm^{-1} of the HA, nor of the vibrations of the HPC hydroxyl groups. This result suggests a lack of hydrogen bonds between the two polymers. Nevertheless it is known that HA reacts, by hydrophobic interactions, with the core protein present in connective tissue.[1]

With this in mind we investigated HA and HPC hydrophobic interactions using Raman spectroscopy. In the region of the stretching vibration of CH groups (Figure 8a), the disappearance of the HPC band at 2985 cm^{-1}, like the modification of the profile of the band at 2900 cm^{-1}, is already observed in the blend containing 10% HA. Starting with the 50/50 HPC/HA mixture, there is at the same time a reduction in the intensity of the HPC bands at 2972 and 2878 cm^{-1} (asymmetric and symmetric stretching of the CH_3 groups, the latter being superimposed by the stretching of CH groups in the glucosidic rings). Further variations in the spectra can be seen in the region of the CH deformations (Figure 8b) where the HPC weak bands at 1319 and 1303 cm^{-1}, most likely due to OH vibrations superimposed by the CH vibrations of the side groups, already disappear with the 10/90 HPC/HA blend. After blending with HA, there are variations not only in frequency but also in intensity of the HPC bands at 1160−1000 cm^{-1} due to deformations ν(C−O−C) of the glucosidic ring and the lateral chains together with deformations and ν(C−O) of the

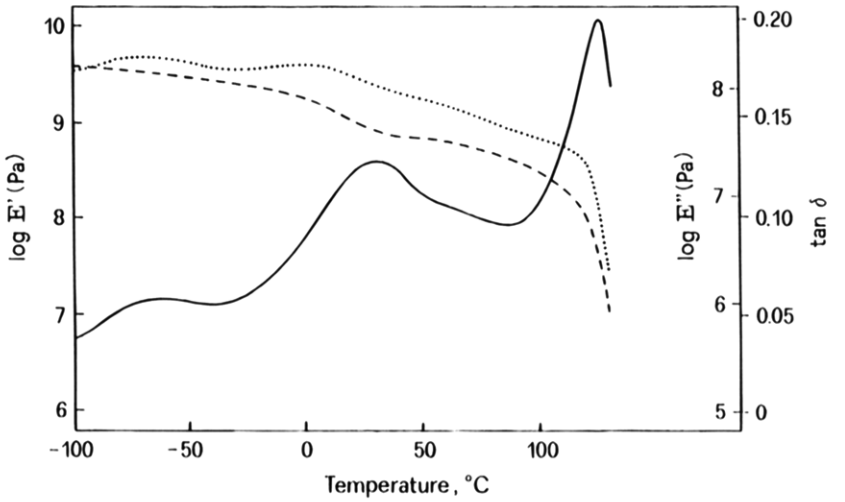

Figure 6. Dynamic mechanical spectrum of dried HPC: (—) tan δ; (- - -) log E'; (•••) log E'').

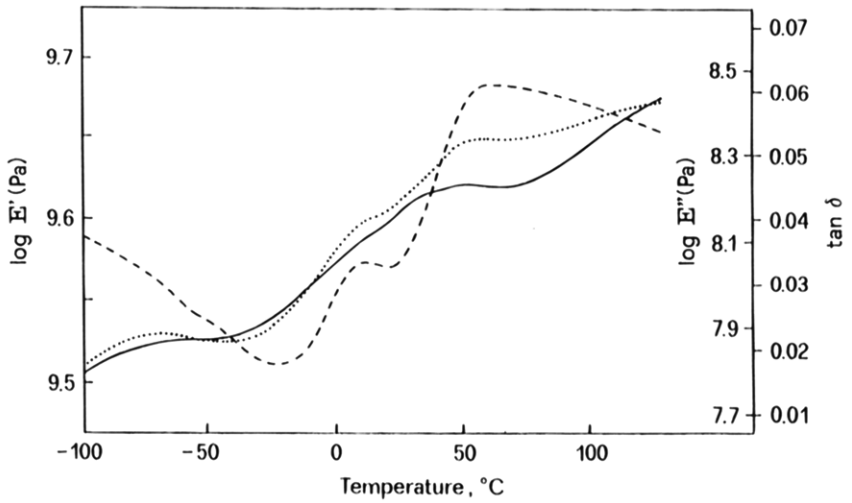

Figure 7. Dynamic mechanical spectrum of dried HA: (—) tan δ; (- - -) log E', (•••) log E'').

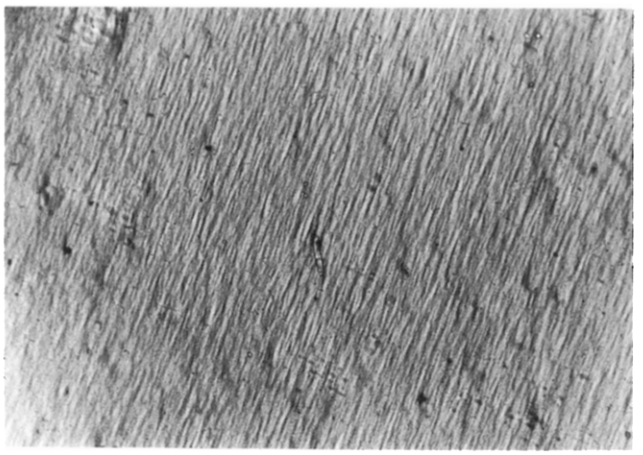

Photo 3. Optical micrograph of the texture of the 75/25 HPC/HA blend at 180 °C.

Photo 4. Optical micrograph of the texture of the 90/10 HPC/HA blend at 180 °C.

lateral chains. Furthermore, while the band at 1159 cm^{-1} disappears, there is the appearance of a new band at 1090 cm^{-1} (Figure 8b). Finally, an examination of the spectrum at 950−750 cm^{-1}, a region highly sensitive to conformational variations of the polysaccharide backbone, shows the complete disappearance of the bands of HPC and HA at 964 and 896 cm^{-1}, respectively, and variations in the intensity of other bands in the spectrum. The variations in frequency and intensity of the Raman bands, especially those localized in the regions more sensitive to conformational variations, though not easily attributable to specific interactions between the two polymers functional groups, seem to suggest a certain number of interactions at the level of the polymer chain segments, the number and strength of such polymer interactions depending on the composition of the blend.

The compatibility of two semicrystalline polymers seldom involves their more ordered regions. As expected, the HPC/HA blends showed no new reflections

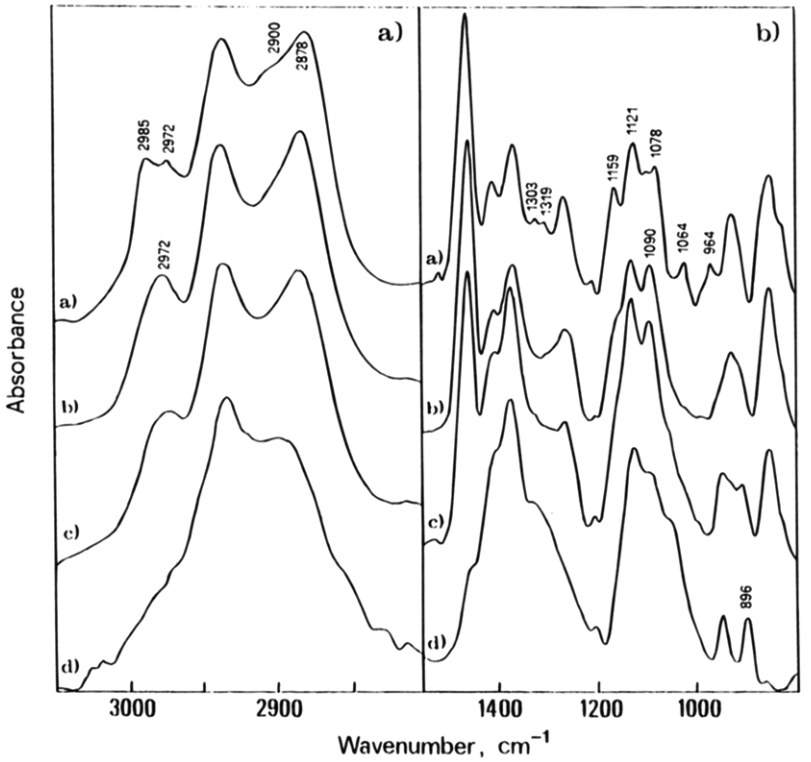

Figure 8. Raman spectroscopy of HPC/HA blends: (a) 100/0; (b) 90/10; (c) 50/50; (d) 0/100).

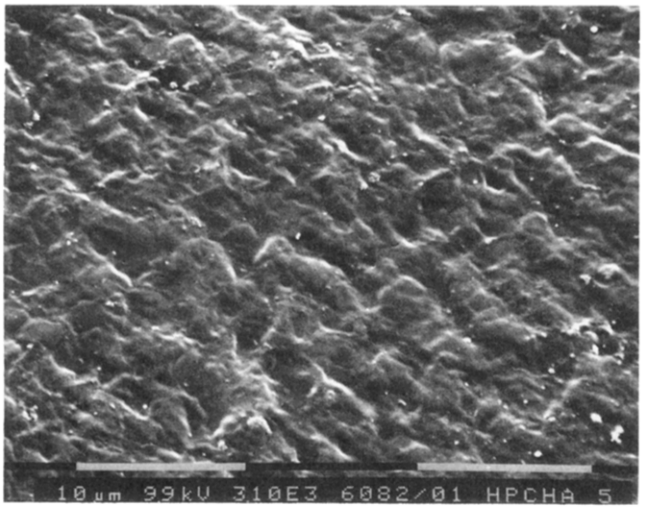

Photo 5. SEM of the 25/75 HPC/75HA blend.

in the X-ray diffractograms (not shown), suggesting that possible interactions can almost exclusively involve the less ordered region of the single components, such regions being particularly abundant in unstretched film where there is a reflection due to superimposed phases of low regularity.

The electron microscope observations (Photo 5) of films prepared from solutions of overall polymer concentration less than C_p' did not show any phase separation (within the micron size range) regardless of the blend composition, confirming a certain degree of compatibility between the two polymers in the solid state.

For a greater insight into HPC/HA compatibility DMTA measurements were used to evaluate the vitreous transition temperature of mixtures of different compositions (Figure 9). The storage modulus E' of the HPC/HA blends (Figure 9a) generally shows an intermediate behavior between the two blend components while the tan δ peak (Figure 9b) shifts to a lower

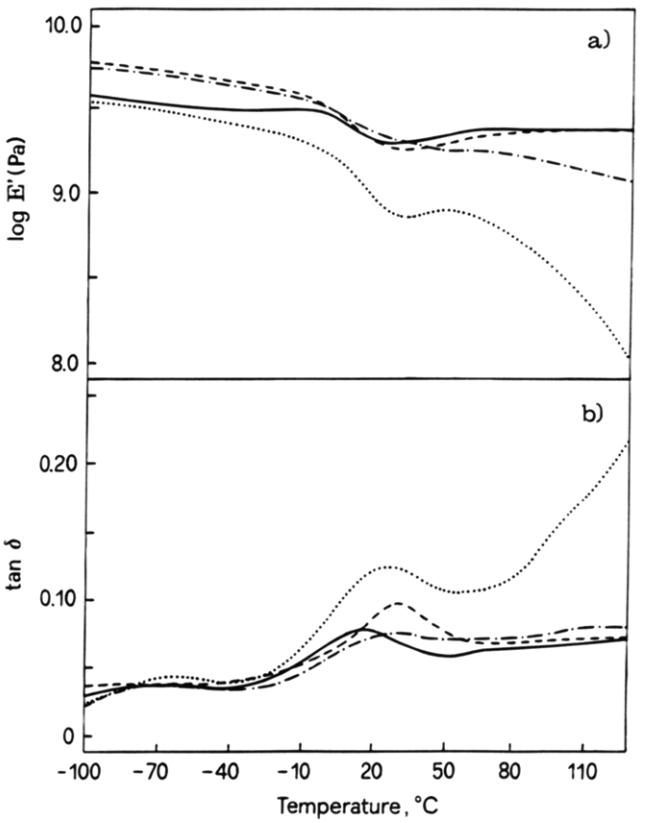

Figure 9. Dynamic mechanical spectrum of HPC/HA dried blends: (—) 10/90; (- - -) 25/75; (• – •) 50/50; (•••) 90/10.

temperature on increasing the HA content. As reported in the literature,[39] there is only one vitreous transition for compatible polymers, generally intermediate to that of the individual components in the HPC/HA mixture (Figure 10). It follows that the HPC/HA system is homogeneous both in the amorphous phase (HA > 50%) and in the liquid crystalline phase, suggesting that HA

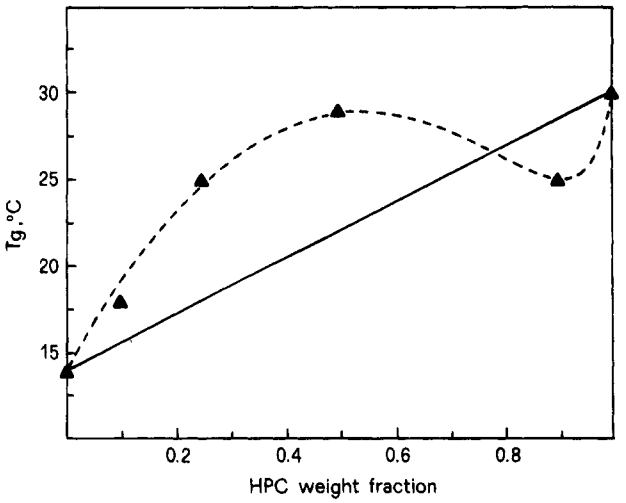

Figure 10. Glass transition temperature of HPC/HA dried blends: (▲) experimental point; (- - -) theoretical trend; (—) weight-average values.

behaves as a solvent, inducing a transition from a liquid crystalline phase to an isotropic one when the HA content increases.

The literature makes reference to several empirical equations to correlate the T_g value of a miscible blend with its compositions, giving some parameters that allow the estimation of the interaction strength between the components.[39-41] As shown in Figure 10 the T_g values versus the composition curve of HPC/HA blends follows, for the dried blend films, as S-shaped curve well fitted by the Kwei equation:[41]

$$T_g = \frac{w_1 T_{g1} + k w_2 T_{g2}}{w_1 + k w_2} + q w_1 w_2$$

where w_1, w_2 and T_{g1}, T_{g2} are the weight fractions and glass transition temperatures of HPC and HA, respectively. The first term of the equation is the classical Gordon–Taylor[40] equation and represents the mixing term derived by using the additive rule of the entropy or of the volume of the blend. The quadratic term (qw_1w_2) is proportional to the number of interactions between the components, most of them interpreted as hydrogen bonds. Both the k value from Gordon–Taylor and the q from the Kwei equation are used in the literature to estimate the strength of the interchain interactions.[41] A good fitting of the experimental data has been found for values of $k = 15$ and $q = 55$, indicating interactions between the polymers, as observed by Raman experiments.

Several experiments were also carried out on conditioned films (65% RH) of HPC, HA, and their blends. Generally, all the transitions observed on such samples are shifted to a slightly lower temperature and energy, revealing the plasticizer effect of water. In particular the higher slope of the curve of the storage modulus E' vs temperature highlights the important role of water on the phenomena associated with large-scale motions of molecular chain segments such as T_g events (Figure 11). In the case of conditioned films of HPC/HA blends, the T_g values versus the composition curve follow a monotonic function, fitting well with the Kwei equation where $k = 1$ and $q = 10$ (Figure 12). Very small positive deviations from weight-average values are observed. Due to the low q value, such deviations show that the interactions between the two polymers in conditioned samples are weaker than in dry polymers.[42,43] It is very likely that in the conditioned samples the water interacts strongly with the two polymers, interposing itself between the polymer molecules and reducing the intermolecular interactions; thus the higher the water content in the mixture the lower the interaction.

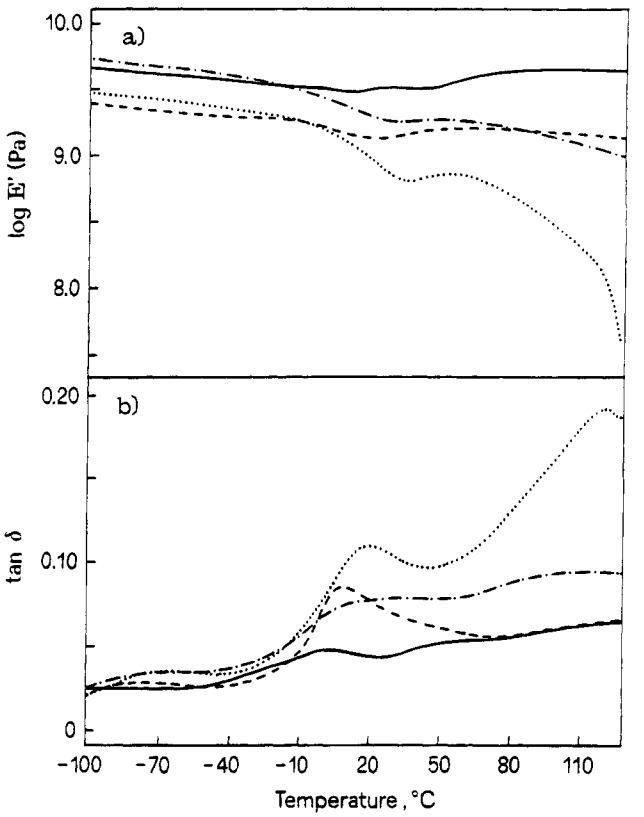

Figure 11. Dynamic mechanical spectrum of HPC/HA conditioned blends: (—) 10/90; (- - -) 25/75; (• — •) 50/50; (• • •) 90/10.

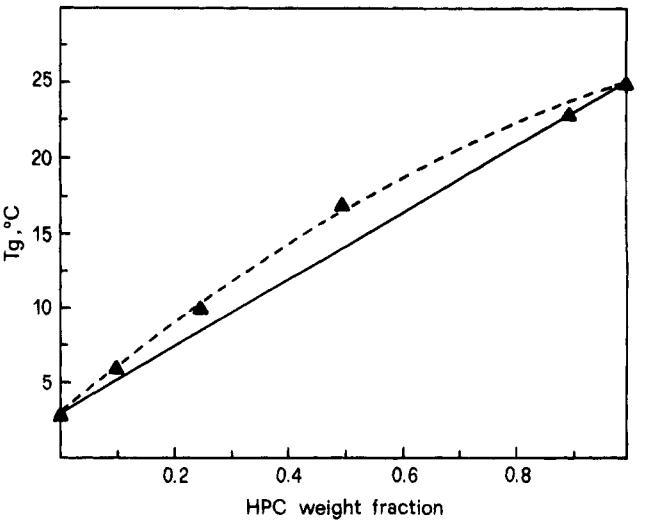

Figure 12. Glass transition temperature of HPC/HA conditioned blends: (▲) experimental points; (- - -) theoretical trend; (—) weight-average values.

Concluding Remarks

It is not easy to explain the complete compatibility of two solid state polymers that, in solution, are incompatible. A possible kinetic interpretation is based on the fact that the evaporation rate of the solvent from the homogeneous dilute solution could be faster than the separation rate of the polymers into two stable phases;

this would "freeze" the polymers in a homogeneous but metastable phase.[44] If films obtained in this way were subjected to a subsequent thermal treatment at temperatures higher than the polymer glass transition, a more stable thermodynamic state would be reached following the demixing of the two polymers. Such a separation should be easily observed, but this was not the case of HPC/HA films treated for long periods (48 h) at temperatures higher than T_g (60 °C).

The theory of phase behavior of flexible polymer blends predicts the possible existence of systems showing a homogeneous phase in the solid state but phase separation in solution.[45,46] This may happen when the interactions between the two polymers are totally favorable or, at least, not unfavorable ($\chi_{23} \leq 0$ or χ_{23} slightly >0) to exceed the entropic gain due to the blending, and the interaction between the polymers and the solvent are very strong (χ_{12} and $\chi_{13} < 0$). In such a case the adding of a solvent to the homogeneous blend of the two polymers leads to a separation into two phases, each stabilized by the polymer–solvent interaction that is stronger than the one between the two macromolecular compounds; in a dilute solution it is possible to again obtain a homogeneous system. When one of the components of the system is rigid or semirigid, like HPC in our case, even though the interaction between the polymers is null ($\chi_{23} = 0$) the theory predicts a phase separation due to the entropic loss that would follow the mixing of the liquid crystal with the flexible polymer.[21] This happens because the flexible polymer disturbs the high orientation of the rigid one in the liquid crystalline phase; in this situation only a strong and favorable interaction between the two polymers ($\chi_{23} < 0$) could counteract the opposing entropic factor. In our system, the results of the Raman spectra and the values of the k and q parameters, obtained according to the Kwei method from the interpolation of experimental T_g values vs composition, seem to indicate some polymer interactions; furthermore the χ_{12} and χ_{13} parameters for HPC/H_2O and HA/H_2O should also be less than zero. In fact strong interactions between HPC or HA and water are predictable and we observed a marked decrease in k and q values when conditioned films were used. It can thus be supposed that in a HA/HPC/H_2O system a situation similar to that theoretically predicted for flexible polymers is established, there being complete compatibility in the solid state whereas in solution there is separation into two phases due to the higher affinity the two polymers show for the solvent, rather than to an incompatibility between them. Moreover the formation of a liquid crystalline phase would contribute to the observed incompatibility. The combined effect of these two factors can explain the phase behavior of our system. We believe that this interpretation, though only speculative, is sounder than the kinetic one.

Acknowledgment. We thank Prof. R. St. J. Manley for a critical reading of the manuscript and useful comments. We thank Ms. M. T. Palma and Ms. V. Richter for their help in obtaining optical micrographs and Raman spectra. Discussions with Dr. A. Francescangeli and Dr. W. Porzio are appreciated. We are grateful for the support of this project through the "Progetto Finalizzato Chimica Fine II" of CNR (Contract No. 93.02920.PF72).

References and Notes

(1) Comper, W. D.; Laurent, T. C. *Physiol. Rev.* **1978**, *58*, 255.
(2) *The Biology of Hyaluronan*; Ciba Foundation Symposium 143; John Wiley & Sons Publishers: New York, 1989.
(3) Laurent, T. C. *Abstracts of the 2nd Joint Meeting on Carbohydrates*; Centro Ricerche POLY-bios Publs-Trieste-Grado, May 28–30, 1992; p 11.
(4) Heatley, F.; Scott, J. E. *Biochem. J.* **1988**, *254*, 489.
(5) Balasz, E. A.; Leshchiner, E. A. In *Cellulosic Utilization, Research and Rewards in Cellulosics*; Inagaki, H., Phillips, G. O., Eds.; Elsevier Applied Science Publishers: London and New York, 1989; p 233.
(6) Della Valle, F.; Romeo, A. U.S. Patent 4,851,521, July 25, 1989.
(7) Bianchi, E.; Ciferri, A.; Tealdi, A. *Macromolecules* **1982**, *15*, 1268.
(8) Conio, G.; Bianchi, E.; Ciferri, A.; Tealdi, A.; Aden, M. A. *Macromolecules* **1983**, *16*, 1264.
(9) Ghosh, S.; Li, X.; Reed, C. E.; Reed, W. F. *Biopolymers* **1990**, *30*, 1101.
(10) Fouissac, E.; Milas, M.; Rinaudo, M.; Borsali, R. *Macromolecules* **1992**, *25*, 5613.
(11) Rinaudo, M.; Milas, M.; Jouon, N.; Borsali, R. *Polymer* **1993**, *34*, 3710.
(12) Odijk, T.; Houwaart, A. C. *J. Polym. Sci. Polym. Phys. Ed.* **1978**, *16*, 627.
(13) Cleland, R. L. *Biopolymers* **1984**, *23*, 647.
(14) Terbojevich, M.; Carraro, C.; Cosani, A.; Marsano, E. *Carbohydr. Res.* **1988**, *180*, 73.
(15) Carpaneto, L.; Marsano, E. *Polym. Bull.* **1994**, *32*, 719.
(16) Flory, P. J. *Adv. Polym. Sci.* **1984**, *59*, 1.
(17) Marsano, E.; Bianchi, E.; Ciferri, A.; Ramis, G.; Tealdi, A. *Macromolecules* **1986**, *19*, 626.
(18) Marsano, E.; Bianchi, E.; Ciferri, A. *Macromolecules* **1984**, *17*, 2886.
(19) Marsano, E. *Polymer* **1986**, *27*, 118.
(20) Barton, A. *Handbook of Solubility Parameters and other Cohesion Parameters*; CRC Press Inc.: Boca Raton, FL, 1983.
(21) Matheson, R. R.; Flory, P. J. *Macromolecules* **1981**, *14*, 954.
(22) Werbowyj, R. S.; Gray, D. G. *Macromolecules* **1980**, *13*, 69.
(23) Dayan, S.; Gilli, J. M.; Sixou, P. *J. Appl. Polym. Sci.* **1983**, *28*, 1527.
(24) Aden, M. A.; Bianchi, E.; Ciferri, A.; Conio, G.; Tealdi, A. *Macromolecules* **1984**, *17*, 2010.
(25) Ciferri, A.; Marsano, E. *Gazz. Chim. Ital.* **1987**, *117*, 567.
(26) Mitchell, G. R.; Guo, W.; Davis, F. J. *Polymer* **1992**, *33*, 68.
(27) Piculell, L.; Nilsson, S.; Falk, L.; Tjerneld, F. *Polym. Commun.* **1991**, *32*, 158.
(28) Samuels, R. J. *J. Polym. Sci., Polym. Chem. Ed.* **1969**, *7*, 1197.
(29) Francescangeli, O.; Marsano, E.; Focher, B. Unpublished results.
(30) Pizzoli, M.; Scandola, M.; Ceccorulli, G. *Plast. Rubber Compos. Process. Appl.* **1991**, *16*, 299.
(31) Rials, T. G.; Glasser, W. G. *J. Appl. Polym. Sci.* **1988**, *36*, 749.
(32) Nishio, Y.; Manley, R. St. J. *Macromolecules* **1988**, *21*, 1270.
(33) Masson, J. F.; Manley, R. St. J. *Macromolecules* **1991**, *24*, 5914.
(34) Masson, J. F.; Manley, R. St. J. *Macromolecules* **1991**, *24*, 6670.
(35) Bradley, S. A.; Carr, S. H. *J. Polym. Sci., Polym. Phys. Ed.* **1976**, *14*, 11.
(36) Atkins, E. D. T.; Meader, D.; Scott, J. E. *Int. J. Biol. Macromol.* **1980**, *2*, 318.
(37) Mitra, A. K.; Arnott, S.; Sheehan, J. K. *J. Mol. Biol.* **1983**, *169*, 813.
(38) Giusti, P.; Lazzeri, L.; Barbani, N.; Lelli, L.; Palla, M.; Narducci, P. *Abstracts of the Fourth European Symposium on Polymer Blends*; IRTEMP Publishers, CNR, Naples, Capri (Italy), May 24–26, 1993; p 65.
(39) Aubin, M.; Prud'homme, R. E. *Macromolecules* **1988**, *21*, 2945.
(40) Gordon, M.; Taylor, J. S. *J. Appl. Chem.* **1952**, *2*, 495.
(41) Kwei, T. K. *J. Polym. Sci. Polym. Lett. Ed.* **1984**, *22*, 307.
(42) Kalichevsky, M. T.; Jaroszkiewicz, E. M.; Ablett, S.; Blanshard, J. M. V.; Lillford, P. J. *Carbohydr. Polym.* **1992**, *18*, 77.
(43) Orford, P. D.; Parker, R.; Ring, S. G.; Smith, A. C. *Int. J. Biol. Macromol.* **1989**, *11*, 91.
(44) Marsano, E.; Tamagno, M.; Bianchi, E.; Terbojevich, M.; Cosani, A. *Polym. Adv. Technol.* **1993**, *4*, 25.
(45) Hsu, C. C.; Prausnitz, J. M. *Macromolecules* **1974**, *7*, 320.
(46) Zeman, L.; Patterson, D. *Macromolecules* **1972**, *5*, 513.

MA945031R